2014 IEEE International Conference on Fuzzy Systems (FUZZ-IEEE)
July 6-11, 2014, Beijing, China

Ocular Artifact Removal from EEG Using ANFIS

Wei Chen, Ze Wang, Ka Fai Lao and Feng Wan
Department of Electrical and Computer Engineering
Faculty of Science and Technology, University of Macau
E-mail: fwan@umac.mo

***Abstract*—Electroencephalogram (EEG) signals are often contaminated with various artifacts, especially electrooculogram (EOG) or ocular artifacts that cannot be avoided consciously and largely degrade the clinical interpretation of the signals. This paper presents a study on adaptive noise cancellation (ANC) based on adaptive neuro-fuzzy inference system (ANFIS) for EOG artifacts removal, especially when time delay is significant and on real contaminated EEG signal. The performance is first evaluated using simulated EEG and EOG signals, further investigation on the effect of time delay and tests on real data are also performed. The results illustrate that ANFIS provides a promising approach to ocular artifact removal with the best performance in comparison with ANC using adaptive filtering and ADALINE.**

***Keywords*—EOG artifact removal; EEG; ANFIS; adaptive noise cancellation; time delay**

I. INTRODUCTION

Electroencephalogram (EEG) is a non-invasive measurement of the electrical activity of the brain obtained electrodes placed on the scalp over multiple areas of the brain. However, as an important clinical tool in the diagnosis and management of neurological disorders, EEG is often affected by a variety of signal contaminations or artifacts, which impairs its clinical usefulness or the diagnosis accuracy. Apart from external artifacts caused by electrodes and alternating current supply to the equipment, major biological artifacts may contain EOG (eye blinks and eyeball movements), ECG (cardiac rhythms) and EMG (face or head muscle artifacts) [1].

The influence of external artifacts can be reduced to a large degree by improving technology and paying extra attention to the attachment of electrodes to the scalp, and some of the biological artifacts may be avoided if the subject follows appropriate guidelines [2]. For the others, however, especially the ocular artifacts which are of elevated amplitudes and may overlap spectrally with EEG signals, automated artifact detection and removal techniques are the most practical solutions. For this purpose, different techniques have been introduced in the last two decades.

To remove the artifacts from EEG, many regression-based methods [3, 4], either in the time domain or in the frequency domain, have been proposed. Regression-based methods are able to reduce ocular artifacts with good performance. In all the regression-based approaches, calibration trials are first conducted to determine the transfer coefficients between the EOG channel and EEG channel, which are later used in the correction phase to estimate the artifacts component in the EEG recording for removal by subtraction [5]. That is to say, all these methods require off-line analysis and thus are not suitable for real-time applications.

Another class of EOG removal methods are component-based, based on for instance principal component analysis (PCA) and independent component analysis (ICA). The limitation of PCA-based methods is the prior assumption that the decomposed components are algebraically orthogonal, which is generally difficult to fulfill [6]. It was also reported that PCA cannot completely separate ocular artifacts from EEG signals, especially when they have comparable amplitudes [7]. For the more recent ICA method, however, it requires visual inspection of ICA components and manual classification of the interference components, which is time-consuming and thus also not desirable for real-time artifacts cancellation [8].

Ocular artifacts removal methods based on wavelets have been proposed in [9, 10].The idea of these denoising methods relies on the assumption that the magnitude of the signals dominates that of the artifacts in wavelet representation. Basically, filtering is performed by comparing each wavelet coefficient to a predetermined threshold and setting it to zero if its magnitude is less than the threshold. The main difficulty in artifacts removal problem is to select a proper threshold level so that it exactly removes the artifacts while keeping the original EEG signals intact.

This study investigate adaptive noise cancellation (ANC) [11] using adaptive neuro-fuzzy inference system (ANFIS) [12] for ocular artifacts removal from EEG. Simulated signals are used to test and evaluate its performance and ANC using adaptive filtering [13] and adaptive linear neuron (ADALINE) [14] is also tested as comparison. Most importantly, further analysis and real data tests about the influence of time delay contained in the signal are performed.

II. METHODOLOGY

A. Adaptive Noise Cancellation (ANC)

The objective of ANC is to filter out interference components by identifying a model between a measurable noise source and the corresponding immeasurable

This work was supported in part by the Macau Science and Technology Development Fund under Grant FDCT 036/2009/A and the University of Macau Research Committee under Grants MYRG139(Y1-L2)-FST11-WF, MYRG079(Y1-L2)-FST12-VMI, MYRG069(Y1-L2)-FST13-WF and MYRG2014-00174-FST.

interference contained in the measured signal [14]. The scheme has a corrupted signal as the primary input and a reference input that consists of noise correlated in some unknown way with the primary noise. It is assumed that the desired clean signal is uncorrelated with the noise source and interference signals. By adaptively filtering and subtracting the reference input from the primary input, the denoised signal will be an estimate of the clean signal. Fig. 1 [15] shows the adaptive noise cancellation (ANC) scheme.

The reference input to the canceller, which is the input to the adaptive filter, is the noise source signal, $n(k)$, measured directly from the artifact generating origin. It goes through the unknown nonlinear dynamics $f(.)$ (i.e. the route in human body from the artifact generating source to each EEG electrode on the scalp) and generates a distorted noise $d(k)$, which is then added to the clean EEG signal $x(k)$ to form $y(k) = x(k)+d(k)$, the measured signal at the EEG electrodes. In another path, the noise $n(k)$ is filtered to produce $\hat{d}(k)$ as close a replica as possible of the interference signal, $d(k)$, which is the distorted and delayed version of $n(k)$. The aim is to retrieve clean EEG, $x(k)$, from the measured EEG signal, $y(k)$, by estimating $\hat{d}(k)$ using the adaptive filter, which is then subtracted from the measured signal $y(k)$ to produce the output of the system, $\hat{x}(k)$, which would be close to the desired signal $x(k)$.

In the noise removal applications, the objective is to produce an "error" signal $\hat{x}(k)$ (system output) that is a best fit in the least squares sense to the signal $x(k)$. This is accomplished by feeding back the system output to the adaptive filter to minimize the "error" signal until it reaches the value, i.e. $\hat{x}(k) = x(k)$. As a result, the output of the noise canceller $\hat{x}(k)$ is the estimation of the clean EEG:

$$\hat{x}(k) = x(k) + d(k) - \hat{d}(k) \tag{1}$$

Squaring both sides leads to

$$\hat{x}(k)^2 = x(k)^2 + [d(k) - \hat{d}(k)]^2 + 2x(k)[d(k) - \hat{d}(k)] \tag{2}$$

Taking the expected value for both sides, and assuming that $x(k)$ is uncorrelated with $n(k)$ and $d(k)$ and thus with $\hat{d}(k)$:

$$\begin{aligned} E[\hat{x}(k)^2] &= E[x(k)^2] + E[[d(k) - \hat{d}(k)]^2] \\ &\quad +2E[x(k)[d(k) - \hat{d}(k)]] \\ &= E[x(k)^2] + E[[d(k) - \hat{d}(k)]^2] \end{aligned} \tag{3}$$

Since the signal power $x(k)^2$ is a specific value, the minimum output power will be given by

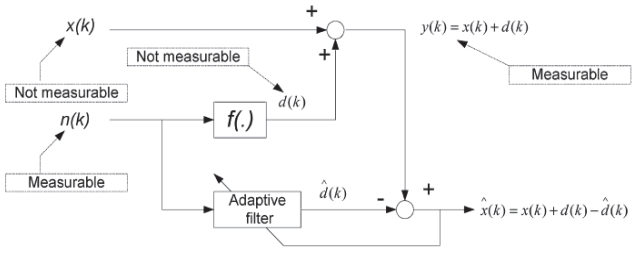

Fig. 1. Block diagram of ANC

$$\min E[\hat{x}(k)^2] = E[x(k)^2] + \min E[[d(k) - \hat{d}(k)]^2] \tag{4}$$

Therefore, when the filter is adjusted so that $E[\hat{x}(k)^2]$ is minimized, $E[[d(k) - \hat{d}(k)]^2]$ is also minimized. The filter output $\hat{d}(k)$ is then the best least squares estimate of the interference signal $d(k)$. With considering

$$E[[x(k) - \hat{x}(k)]^2] = E[[d(k) - \hat{d}(k)]^2] \tag{5}$$

the output signal $\hat{x}(k)$ will also be the best least squares estimate of the clean EEG signal $x(k)$

$$\hat{x}(k) \approx x(k) \tag{6}$$

It should be noted that it may take some time for artifact signal to reach the EEG electrodes on the scalp from its origin, which results in a delay between the artifact generation time and the time it contaminates the EEG signal. Therefore, to consider this delay possibility, a tapped delay line (TDL) can be used for the noise source signal [2]. Fig. 2 shows the structure that the noise source signal passes through the TDL before going into the adaptive filter. The noise source signal passes through r-1 delays. The output of the TDL, which is the input of the adaptive filter, is an r-dimensional vector, $X(k) = [x_1(k) \quad x_2(k) \quad \cdots \quad x_r(k)]^T$, made up of the noise source signal at the current time and the previous ones.

The adaptive noise cancellation (ANC) scheme is flexible, since the adaptive filter within the scheme can be implemented using different methods (e.g. adaptive filtering, ADALINE and ANFIS in this study).

B. Adaptive Neuro-Fuzzy Inference System (ANFIS)

ANC using linear filters (i.e. adaptive filtering) has been used widely and successfully in real world applications such as noise cancellation for EEG and ECG signals, echo elimination on long distance telephone transmission lines and antenna side lobe interference removal [16]. Moreover, when facing increasingly complex systems, the concept of linear adaptive noise cancellation can be extended to nonlinear realms by using nonlinear adaptive filters, one of which is the adaptive neuro-fuzzy inference system (ANFIS) introduced by Roger Jang in 1993.

The ANFIS is a combination of fuzzy inference system and artificial neural networks, taking advantages of both

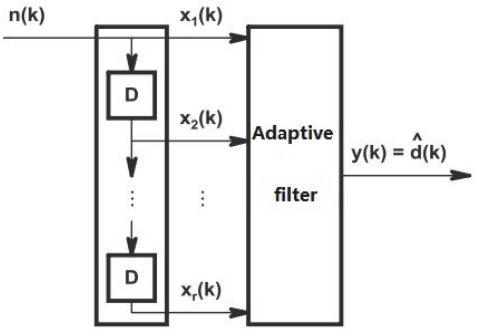

Fig. 2. Applying TDL to the input of the adaptive filter

powerful techniques. More specifically, neural networks recognize patterns by its outstanding learning capability and facilitate adaptation to the changing environments. Fuzzy inference systems incorporate human knowledge and perform interfacing and decision-making. The basic idea of ANFIS is to design an architecture that uses a fuzzy system to represent knowledge in an interpretable manner, while possessing the learning capability of neural networks to optimize its parameters [12]. Therefore, this hybrid architecture is able to overcome some of the individual weaknesses and offer appealing nonlinear problem-solving capability.

The basic structure of a fuzzy inference system consists of three conceptual components: a rule base consisting of a selection of fuzzy rules; a database describing the membership functions used in the fuzzy rules; and a reasoning mechanism that derives a reasonable output or conclusion by performing the inference procedure upon the rules and the given facts [12]. The fuzzy reasoning mechanism to derive an output f from the given input vector [x, y] and consequent parameters [p, q, r] is graphically illustrated in Fig. 3 [17]. The product of membership grades in the premise part is usually used to obtain the firing strengths w_1 and w_2, and weighted average of each rule's consequence is the output f. Due to the high interpretability, computational efficiency, built-in optimal and adaptive nature, the Sugeno fuzzy model is the most extensively used one among various FIS models [17].

The learning algorithm tunes the membership functions of a Sugeno fuzzy inference system by using training input-output data. Two inputs x, y and one output f are considered for simplicity. A common rule set with two fuzzy if-then rules for a first order Sugeno fuzzy system can be represented as:

$$\text{If } x \text{ is } A_1 \text{ and } y \text{ is } B_1, \text{ then } f_1 = p_1x + q_1y + r_1 \qquad (7)$$

$$\text{If } x \text{ is } A_2 \text{ and } y \text{ is } B_2, \text{ then } f_2 = p_2x + q_2y + r_2 \qquad (8)$$

Apart from the input and output, ANFIS has five layers. ANFIS architecture is shown in Fig. 4 [17], where a circle represents a fixed node and a square represents an adaptive node (parameters are adjusted during training). Functions of node in each layer of ANFIS are explained as below:

Layer 1: Calculate membership value for premise parameters. Membership grades of a linguistic value are generated by each node of this layer. For instance, a generalized bell membership function can be the node

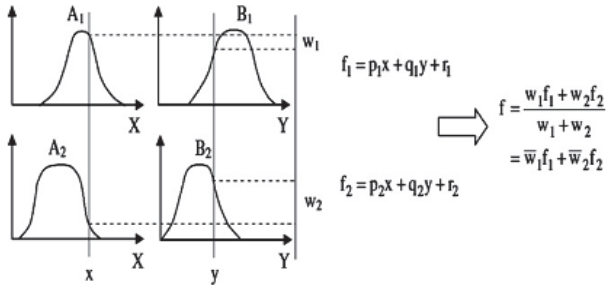

Fig. 3. Two input first order Sugeno fuzzy model

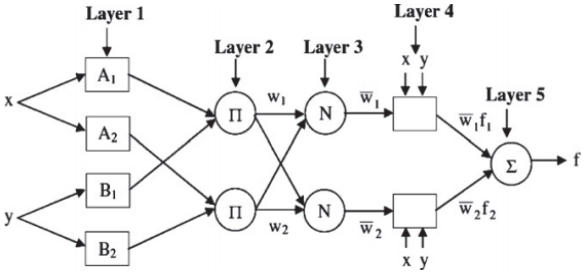

Fig. 4. ANFIS architecture

function of the ith node.

$$O_i^1 = \mu_{A_i}(x) = \frac{1}{1 + \left|(x - c_i)/a_i\right|^{2b_i}} \qquad (9)$$

where x is the input to node i; A_i is the linguistic value of the ith node; and [a_i, b_i, c_i] is the parameter set that alters the shapes of the membership function. Parameters of this layer are called premise parameters.

Layer 2: Generate firing strength of rules. Every node in this layer is a fixed node labeled π. The firing strength of a rule is calculated by each node of this layer through simple multiplication:

$$O_i^2 = w_i = \mu_{A_i}(x)\mu_{B_i}(y), \; i = 1, 2 \qquad (10)$$

Layer 3: Normalize firing strengths. Nodes in this layer are also fixed nodes labeled N. The ratio of the firing strength of the ith rule to the total firing strength is calculated by the ith node of this layer:

$$O_i^3 = \overline{w}_i = \frac{w_i}{w_1 + w_2}, \; i = 1, 2 \qquad (11)$$

Layer 4: Generate consequent parameters. The contribution of ith rule towards the overall output is calculated by the ith node of this layer. Each node in this layer is an adaptive node with node function:

$$O_i^4 = \overline{w}_i f_i = \overline{w}_i (p_i x + q_i y + r_i), \; i = 1, 2 \qquad (12)$$

where $\overline{w}_i$ and [p_i, q_i, r_i] are the output of layer 3 and the parameter set respectively. Parameters of this layer are called consequent parameters.

Layer 5: Produce overall output. The overall output is calculated as the summation of contribution from this rule by the single node of this layer:

$$O_i^5 = \sum_i \overline{w}_i f_i \qquad (13)$$

In this study, we have taken reference noise signal and delayed ones as inputs and the measured corrupted EEG signal as target output for training the ANFIS, which is the same as what we have done for adaptive filtering and ADALINE. ANFIS minimizes the sum of squared error (SSE) by using a hybrid learning algorithm, which combines least squares and back propagation gradient descent methods together. In the forward path, the node outputs go forward until layer 4 and the least squares method is used to

identify the consequent parameters by keeping the premise parameters fixed. In the backward path, the error signals propagate backward and the premise parameters are updated by gradient descent method while keeping consequent parameters fixed.

In this work, all the ANC based methods are used to identify the unknown nonlinear passage dynamics that transforms a noise source into an interference component in the measured EEG signal. Once the adaptive filter yields an estimate of the interference, it is subtracted from the measured signal to retrieve the desired clean EEG signal. All these denoising algorithms were implemented in MATLAB.

III. Results

A. Simulated Signals

To evaluate the performance of each ANC based method while avoiding the effect of other noises besides EOG artifacts, simulated clean EEG, EOG artifacts and corrupted EEG by fusing the above signals were used for the simulation study. For the comparative analysis, signal to noise ratio (SNR), mean square error (MSE) and power spectrum density (PSD) plot were used as performance indexes.

In order to get more information with fewer samples (i.e. 1000 samples), we have made a modification to the proposed signal simulation method [18]. The new autoregressive process for generating EEG signals is given as

$$s(t) = 1.0084s(t-1) - 0.1887s(t-2) - 0.3109s(t-3) - 0.0510s(t-4) + w(t) \quad (14)$$

where $w(t)$ is a white noise sequence with Gaussian distribution.

The artifacts are simulated by an exponentially damped sinusoid with randomly varied amplitudes and shapes satisfying a uniform distribution. The jth artifact is thus simulated as

$$n_j(k) = Ka_j e^{-k/\tau_j} \sin(2\pi k / N), \text{ for k = 0, 1,…, } N\text{-1} \quad (15)$$

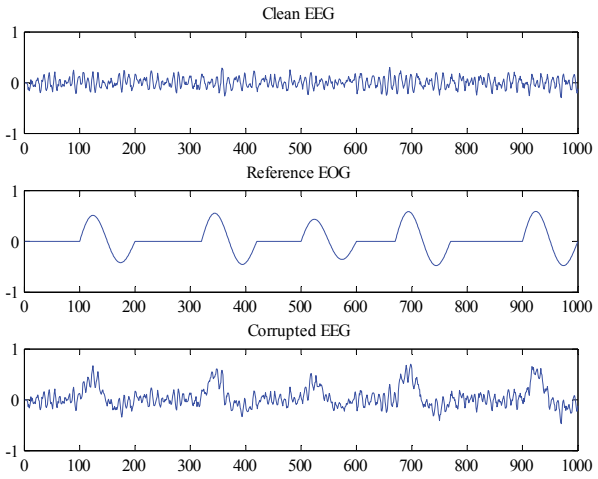

Fig. 5. Simulated signals with a length of 1000 samples

where N is the length of the artifact waveform and is set to 100 samples. The parameter a_j is the amplitude of the jth artifact, τ_j is a parameter determining the shape, and K is an amplitude scaling constant. To simulate the variations in amplitude and shape of the artifacts, both parameters were set to new random values at the onset of each artifact. The new values of a_j and τ_j were randomly chosen from a Gaussian distribution with (μ = 1, σ^2 = 0.1) and (μ = 250, σ^2 = 50), respectively. The artifacts were generated exponentially distributed over time, with the occurrence rate of 0.5 per unit time. One unit time corresponds to 200 samples of discrete time series. The generated artifacts were scaled and added to the simulated clean EEG to provide the primary signal (measured corrupted signal).

In terms of the unknown passage dynamics, we used a nonlinear function to simulate it as the general case. The simulated artifacts were added to the simulated EEG in a nonlinear way to provide the simulated primary signal as

$$x(t) = EEG(t) + \alpha\xi(EOG(t)) \quad (16)$$

where α is a scaling factor, and ξ is the nonlinear transfer, which was chosen to be of the form [19]

$$\xi(EOG(t)) = EOG(t) + EOG^2(t) + EOG^3(t) \quad (17)$$

The simulated signals used in this simulation study are shown in Fig. 5, in which the scaling factor α is selected as 0.5.

B. Simulation Results

For adaptive filtering method, there are two parameters to be determined, namely the filter length M and the forgetting factor λ. Considering the performance, these two parameters were selected to be 3 and 0.9999 respectively, according to [13]. The noise cancellation result is shown in Fig. 6. The error is defined as the difference between the clean EEG and the estimated EEG, as is the same for other simulations.

For ADALINE method, the total number of inputs to the network is chosen to be 4, including the current reference EOG artifact and the previous ones. Simulation tests conclude that more inputs do not improve the noise cancellation performance. The result for ADALINE is shown in Fig. 7. It can be clearly seen that the errors for both methods are still relatively remarkable, since the adaptive filtering method and the ADALINE network are theoretically good choices for only linear problems.

For the ANFIS architecture as shown in Fig. 8, we select the number of inputs as 2 and for each input 3 membership functions, according to [17], which results in 9 fuzzy rules. The generalized bell membership function is used for training in this simulation. The result of noise removal using ANFIS is shown in Fig. 9. The denoising performance is clearly better than those given by the other two methods, since ANFIS is inherently a universal approximator and thus is suitable as a nonlinear filter.

From visual inspection, we have been able to conclude that ANFIS wins over the other two methods (adaptive filtering and ADALINE) in terms of denoising performance. In order to conduct a comprehensive and quantitative

comparative analysis, SNR, MSE and PSD plot are used as performance indexes. SNR is defined as:

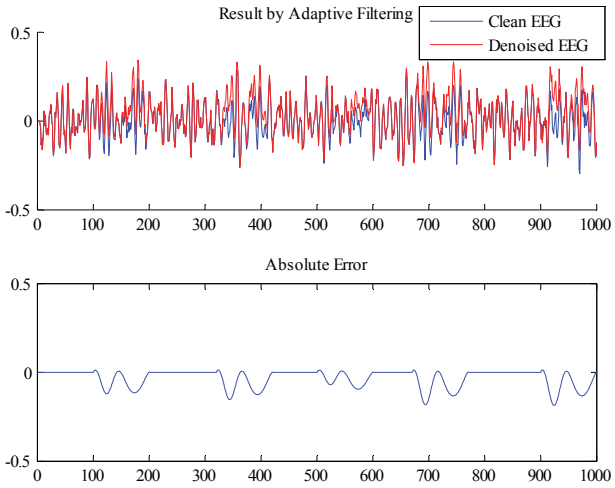

Fig. 6. Simulation result by adaptive filtering

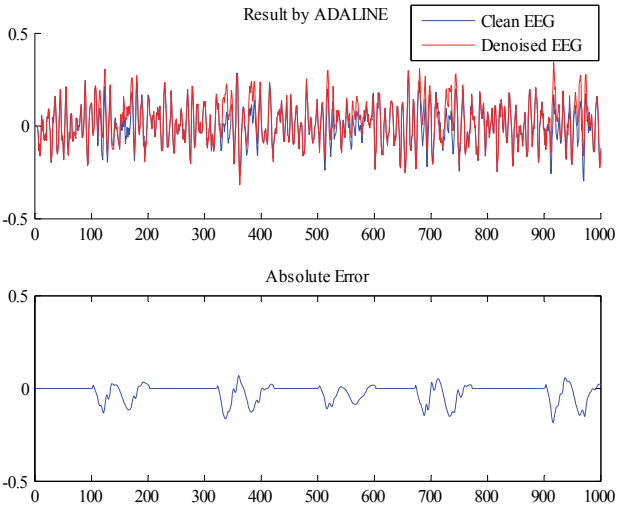

Fig. 7. Simulation result by ADALINE

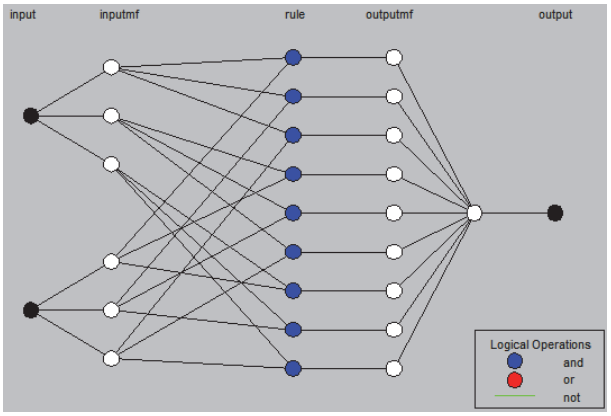

Fig. 8. Structure of ANFIS used in the simulations

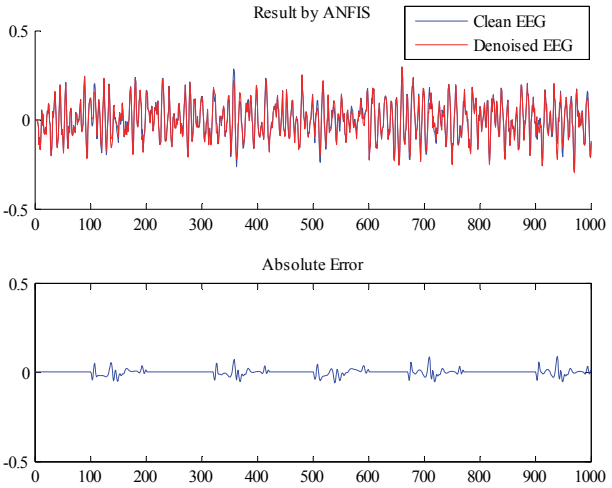

Fig. 9. Simulation result by ANFIS

$$SNR = 10\log_{10}\left(\frac{\sum (E_{eeg})^2}{\sum (S_{eeg} - E_{eeg})^2}\right) \tag{18}$$

where E_{eeg} is the estimated EEG signal and S_{eeg} is the standard EEG signal. The MSE is calculated using the following formula:

$$MSE = \frac{\sum (error)^2}{length(error)} \tag{19}$$

where

$$error = S_{eeg} - E_{eeg} \tag{20}$$

Following the above two index definitions, the corrupted EEG signal has an SNR of 1.2425 and an MSE of 0.0294. The performance analysis for artifact removal using various methods is tabulated in Table 1. It is evident from the results that in this case ANFIS yields the best performance, while ADALINE has a slightly stronger denoising capability than adaptive filtering.

Fig. 10 gives the power spectral density (PSD) plots of various techniques applied to remove EOG artifacts, which is used to show the information about frequency content of the signal and determine the nearness of the extracted signal towards the standard signal. It is clear that ANFIS extracts EEG signal from the primary signal better than adaptive filtering and ADALINE. To conclude, since the dynamics of the channel between EOG source and the primary signal is in fact nonlinear, ANFIS would be the most suitable for the ocular artifact removal application.

TABLE I. PERFORMANCE ANALYSIS FOR VARIOUS METHODS

Methods	SNR (dB)	MSE
Adaptive filtering	6.1543	0.0034
ADALINE	7.2116	0.0025
ANFIS	15.8067	2.6573×10^{-4}

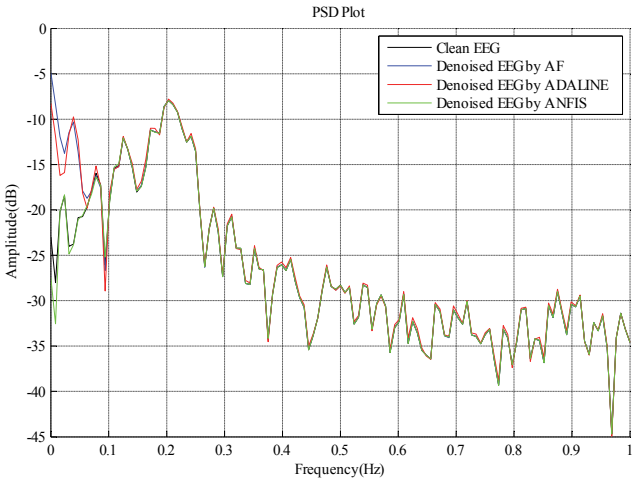

Fig. 10. PSD plots using various techniques

C. Time Delay

It should be noted that the unknown passage between the reference noise and the primary EEG signal is estimated by a nonlinear function without any time delay in our previous simulations, which thus makes ANFIS with only one input may produce the best performance with nearly no error. In practice, always it takes time for the artifact signal to reach the EEG electrodes on the scalp from its origin, leading to a delay between the artifact generation time and the time it contaminates the EEG signal. Therefore, ANFIS with multiple inputs that contain current and previous information achieved by using TDL may yield better results in this case.

However, the effect of time delay has not been mentioned in most related research works. In order to show the effect of time delay, a delay of 10 samples was intentionally added to the nonlinear function that we have used and we used ANFIS with only one input to denoise the signal with time delay. The simulated signal with time delay is shown in Fig. 11 and the result is shown in Fig. 12. When we used ANFIS with two inputs (no other modification), the performance was improved, as shown in Fig. 13. Besides, more inputs

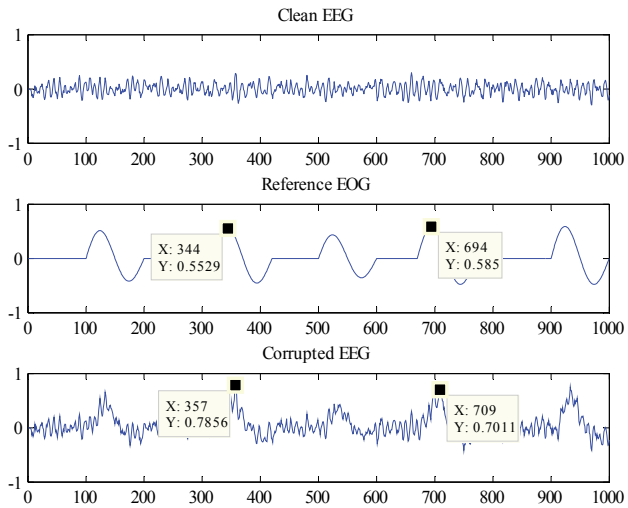

Fig. 11. Simulated signals with a time delay of 10 samples

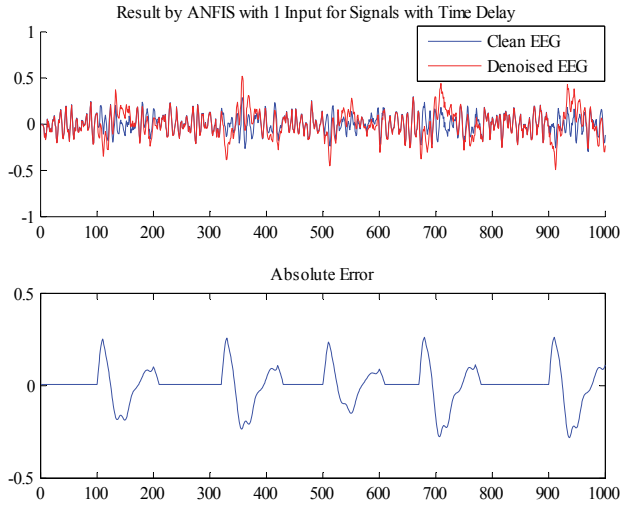

Fig. 12. Result by ANFIS with 1 input for signals with time delay

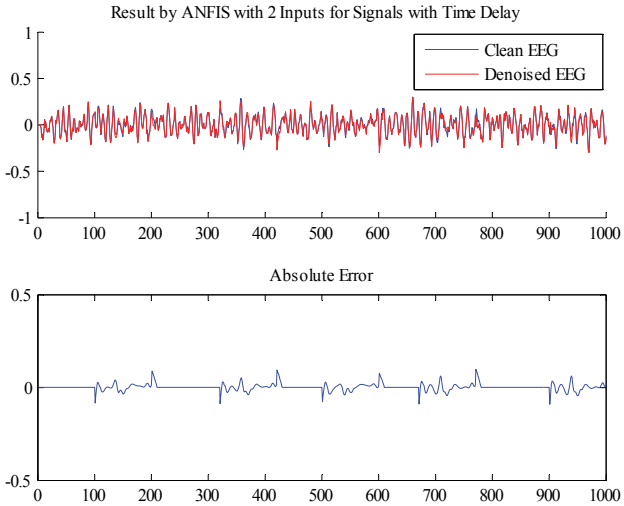

Fig. 13. Result by ANFIS with 2 inputs for signals with time delay

will also result in slight improvement in this simulation at the cost of a longer convergence time.

D. Real Signal Tests

In this section, real signals are used to replace the simulated signals that were used in previous simulation studies. The data with 600 Hz sampling frequency were measured during the SSVEP experiment of one subject in our laboratory. The EEG signal and the EOG signal were measured simultaneously. The real data tests actually contain two parts.

For the first part, we select a length of the standard EEG signal (without ocular artifacts) and EOG signal, both of which has 1800 samples corresponding to 3s in time length. The signals are first normalized and then combined together to obtain the corrupted EEG signal via the nonlinear function (both with and without time delay) that we have mentioned before. The real signals are shown in Fig. 14 and Fig. 15. Two performance indexes (SNR/MSE) of the corrupted EEG signals in two cases are 1.1304/0.0170 and 1.2257/0.0170,

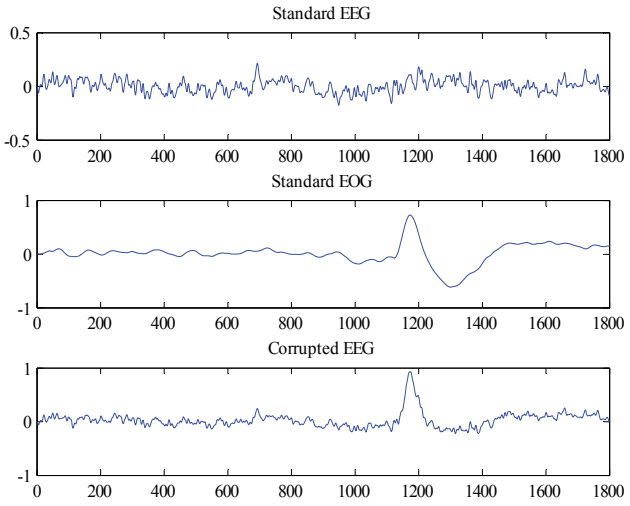

Fig. 14. Real signals without time delay

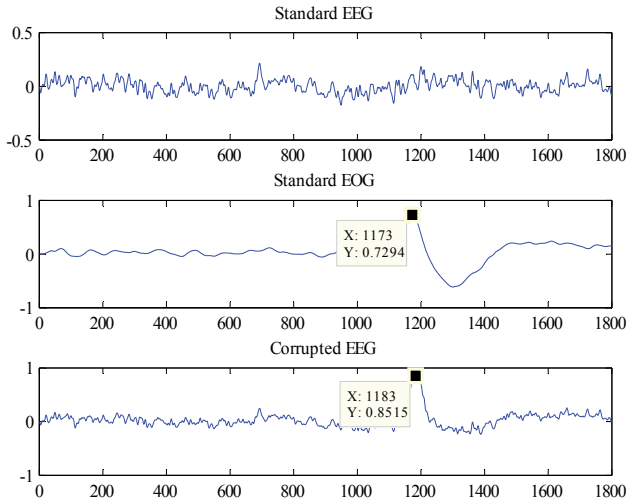

Fig. 15. Real signals with time delay

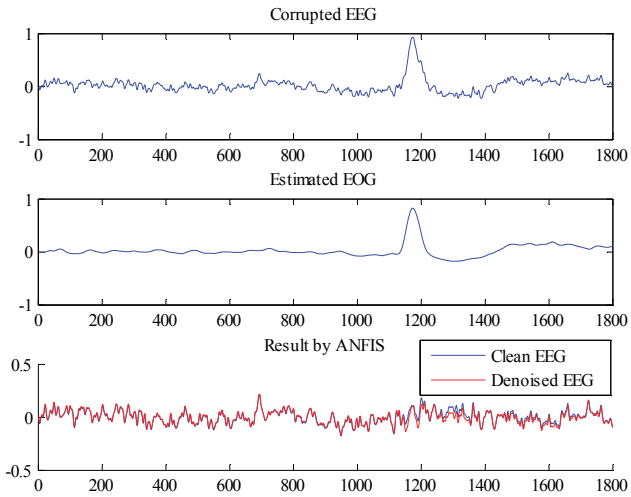

Fig. 16. Result by ANFIS for real signals without time delay

TABLE II. PERFORMANCE ANALYSIS OF ANFIS FOR NON-DELAY CASE

ANFIS Setup		Denoising Performance	
Input number	MF	SNR (dB)	MSE
1	2 gbellmfs	10.6009	3.0767×10^{-4}

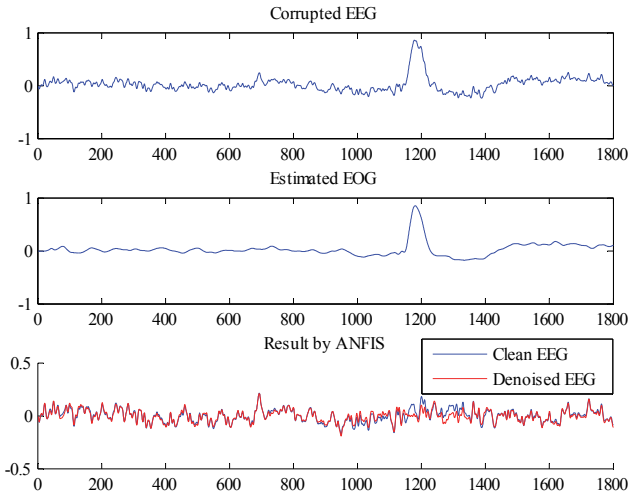

Fig. 17. Result by ANFIS for real signals with time delay

TABLE III. PERFORMANCE ANALYSIS OF ANFIS FOR DELAY CASE

ANFIS Setup		Denoising Performance	
Input number	MF	SNR (dB)	MSE
2	2 gaussmfs	7.6201	5.4642×10^{-4}

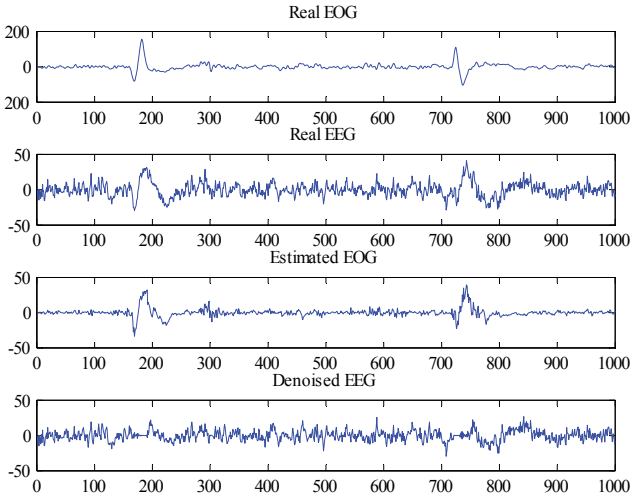

Fig. 18. Result by ANFIS for real field measured signals

respectively. For the case without time delay, ANFIS with one input described by two generalized bell membership functions yields the best performance and the results are shown in Fig. 16. The quantitative result is listed in Table 2. For the case with time, the results by ANFIS with two inputs described by two Gaussian membership functions are shown in Fig. 17. The quantitative result is listed in Table 3.

In both cases, EOG artifacts cannot be entirely removed as was achieved in the cases where simulated signals were used, since real signals are always interfered by the environment and the electrodes and cannot be completely uncorrelated (EOG signals are also contaminated by EEG signals to some extent).

For the second part, we use a length of synchronously field measured EEG signal (inherently with artifacts) and EOG signal, both of which has 9000 samples corresponding to 15s in time length. The signals are first downsampled to 1000 samples to lessen the computational burden. Here the unknown dynamics between the EOG noise source and the measured EEG signal is naturally included in the signals, so we do not need to use a certain function to approximate it as what we have done before. Besides, we also do not have such a standard (clean) EEG as a reference to evaluate the denoising performance by ANFIS that we can only conduct visual inspection, which is the most practical situation. The real signals and the results are shown in Fig. 18.

IV. CONCLUSION

EEG signals are usually contaminated by various artifacts, especially the ocular (EOG) artifacts, which cannot be filtered out effectively by conventional filtering methods due to the spectrum overlap with the desired signal. This research investigates how adaptive noise cancellation (ANC) based on ANFIS works, for EOG artifacts removal from the EEG signal.

The signals used in our first simulation are simulated by a modified autoregressive process and the unknown channel between the reference noise signal (ocular artifact source) and the primary (measured) EEG signal is approximated by a nonlinear function. The simulation result indicates that ANC using ANFIS yields the best performance while adaptive filtering and ADALINE are found to be not that suitable for the nonlinear task. When time delay exists, it is clear that ANFIS with more than only one input implemented by using a TDL will yield better results.

For real data tests, the performance of ANFIS is relatively sensitive to the number of inputs and membership functions, and Gaussian and generalized bell membership functions are usually more suitable than the others. Given a proper selection of those factors, it is proved that ANFIS can provide a good performance. On the whole, considering the operation time and performance, ANFIS is rather suitable for EOG artifact removal from the EEG signal. Besides, as a universal approximator, ANFIS can be a promising approach for not only removing ocular artifacts from EEG, but other noise cancellation applications as well.

REFERENCES

[1] S.R. Benadis and D. Rielo, EEG Artifacts, eMedicine, 2008, Available from: http://emedicine.medscaple.com/article/1140247-overview.

[2] A. Jafarifarmand and M. Ali Badamchizadeh, "Artifacts removal in EEG signal using a new neural network enhanced adaptive filter," Neurocomputing 103, 2013, pp. 222-231.

[3] R. Croft and R. Barry, "EOG correction: which regression should we use?" Psychophysiology 37 (1), 2000, pp: 123-125

[4] R. Croft and R. Barry, "Removal of ocular artifact from the EEG: a review," Clin. Neurophysiol. 30 (1), 2000, pp. 5-19.

[5] A. Garcés Correa, E. Laciar, H.D. Patiño, and M.E. Valentinuzzi, "Artifact removal from EEG signals using adaptive filters in cascade," J. Phys.: Conf. Ser. 90, 2007, pp. 1-10.

[6] C. Joyce and I. Gorodnitsky, "Automatic removal of eye movement and blink artifacts from EEG data using blind component separation," Psychophysiology 41 (2), 2004, pp. 313-325.

[7] T.P. Jung, S. Makeig, C. Humphries, T.W. Lee, M.J. McKeown, V. Iragui, and T.J. Sejnowski, "Removing electroencephalographic artifacts by blind source separation," Psychophysiology 37 (2), 2000, pp. 163-178.

[8] A. Erfanian and B. Mahmoudi, "Real-time ocular artifact suppression using recurrent neural network for electroencephalogram based on brain-computer interface," Med. Biol. Eng. Comput. 43, 2005, pp. 296-305.

[9] V. Krishnaveni, S. Jayaraman, S. Aravind, V. Hariharasudhan, and K. Ramadoss, "Automatic identification and removal of ocular artifacts from EEG using wavelet transform," Meas. Sci. Rev. 6 (4), 2006, pp. 45-57.

[10] P. Senthil Kumar, R. Arumuganathan, K. Sivakumar, and C. Vimal, "Removal of ocular artifacts in the EEG through wavelet transform without using an EOG reference channel," Int. J. Open Probl. Comput. Sci. Math. 1 (3), 2008, pp. 188-200.

[11] B. Widrow, J.R. Golver, J.M. McCool, J. Kaunitz, C.S. Williams, R.H. Hearn, et al., "Adaptive noise canceling: principles and applications," Proc. IEEE, 63, 1975, pp. 1692-1716.

[12] J.S.R. Jang, "ANFIS: Adaptive Network based Fuzzy Inference System," IEEE Transactions of Systems, Man and Cybernetics 23 (3), 1993, pp. 1493-1499.

[13] P. He, G. Wilson, and C. Russell, "Removal of ocular artifacts from electroencephalogram by adaptive filtering," Med. Biol. Eng. Comput., 42, 2004, pp. 407-412.

[14] J.S.R. Jang, C.T. Sun, and E. Mizutani, Neuro Fuzzy and Soft Computing: A Computational Approach to Learning and Machine Intelligence, Prentice Hall International Inc., 1997.

[15] M.J. Er, Z. Li, H.N. Cai, and Q. Chen, "Adaptive noise cancellation using enhanced dynamic fuzzy neural networks," IEEE Transactions on Fuzzy Systems 13 (3), 2005, pp. 331-342.

[16] C. Kezi Selva Vijila, P. Kanagasabapathy, S. Johnson, and V. Edwards, "Efficient cancellation of artifacts in EEG signal using ANFIS," Int. J. of Soft Comput. 2 (3), 2007, pp. 355-360.

[17] S. Suja Priyadharsini and S. Edward Rajan, "An efficient soft computing technique for extraction of EEG signal from tainted EEG signal," Applied Soft Computing 12, 2012, pp. 1131-1137.

[18] X. Yu, Z. He, and Y.S. Zhang, "Time-varying adaptive filters for evoked potential estimation," IEEE Transactions on Biomed. Eng. 41, 1994, pp. 1062-1071.

[19] F. Rauf and H.M. Ahmed, "New nonlinear adaptive filters with applications to chaos," Int. J. Bifurcation Chaos 7, 1997, pp. 1791-1809.